Article

Current Biology

Barn owl color morphs hunt differently in moonlight

Highlights

- Moonlight changes barn owl hunting behavior in color-dependent ways
- White morphs face the Moon and seek light exposure, while red morphs remain cryptic
- In bright light, only white morphs gain capture rates without reducing strike success
- Natural lightscapes may help maintain conspicuous coloration in nocturnal ecosystems

Authors

Kim Schalcher, Estelle Milliet, Robin Séchaud, Roman Bühler, Bettina Almasi, Paolo Becciu, Alexandre Roulin

Correspondence

kim.schalcher@icloud.com (K.S.), paolo.becciu@vogelwarte.ch (P.B.), alexandre.roulin@unil.ch (A.R.)

In brief

Schalcher et al. find that moonlight changes how barn owls hunt: white males face the Moon and select brighter conditions, whereas red males remain more cryptic. These color-dependent strategies reveal how natural lightscapes can shape predator behavior and maintain conspicuous coloration.

Schalcher et al., 2026, Current Biology *36*, 3077–3087
June 22, 2026 © 2026 The Author(s). Published by Elsevier Inc.
https://doi.org/10.1016/j.cub.2026.05.020

CellPress

Current Biology

CellPress
OPEN ACCESS

Article

Barn owl color morphs hunt differently in moonlight

Kim Schalcher,[1,5,*] Estelle Milliet,[1] Robin Séchaud,[1,2] Roman Bühler,[2] Bettina Almasi,[2] Paolo Becciu,[1,2,3,4,*] and Alexandre Roulin[1,3,4,*]

[1]Department of Ecology and Evolution, University of Lausanne, Building Biophore, 1015 Lausanne, Switzerland
[2]Swiss Ornithological Institute, Seerose 1, 6204 Sempach, Switzerland
[3]Senior author
[4]These authors contributed equally
[5]Lead contact
*Correspondence: kim.schalcher@icloud.com (K.S.), paolo.becciu@vogelwarte.ch (P.B.), alexandre.roulin@unil.ch (A.R.)
https://doi.org/10.1016/j.cub.2026.05.020

SUMMARY

Bright coloration in predators presents a paradox: being highly visible should reduce hunting success, yet vivid colors persist in species that rely on stealth. Camouflage, which minimizes contrast with the background, and startle coloration, where sudden brightness disrupts prey escape, have been proposed to explain this paradox. Barn owls (*Tyto alba*) are polymorphic, ranging from dark reddish to bright white, offering a natural experiment. Using high-resolution biologging, we tracked 69 free-ranging males across 354 nights and recorded 17,600 hunting attempts during chick provisioning. We tested whether plumage color mediates moonlight-dependent hunting behavior and performance. White males reduced exposure under dim conditions but, under bright moonlight, oriented attacks toward the Moon and favored bright periods and unshaded sites throughout the night. Red males showed weaker or no adjustments and remained comparatively cryptic. Although per-attack success did not differ across the lunar gradient, white males achieved higher nightly prey capture rates and shorter foraging bouts under bright moonlight. Together with previous work, these patterns are more consistent with the startle hypothesis than with a pure background-matching scenario, suggesting that conspicuous plumage can be incorporated into a light-dependent hunting strategy and that variation in lunar lightscapes may influence the evolution of animal coloration.

INTRODUCTION

Color shapes life-and-death interactions in nature,[1–5] revealing or concealing animals from both predators and prey.[6–11] Some nocturnal predators almost seem to glow in the dark,[12–14] an apparent conspicuousness that appears counterintuitive: predators are generally expected to remain undetected to avoid alerting prey.[11] Yet species such as the barn owl (*Tyto alba*), highly adapted for stealth with silent flight[15,16] and soundless landings,[17] display brilliant white plumage that reflects ambient light.[18] This raises the question of why such conspicuous coloration would persist in a predator built to avoid detection. The answer may lie in how moonlight reshapes the nocturnal visual world for both predators and prey.

Lunar cycles produce predictable but dynamic shifts in night-time illumination,[19,20] generating fluctuating lightscapes that structure predator-prey interactions,[20,21] foraging strategies,[20,22–24] and communication.[20,24–27] From the prey's perspective, bright moonlight can transform open ground into a "landscape of fear," in which illuminated patches are both risky and difficult to avoid.[20,21] As illumination increases, predators may face new trade-offs: brighter conditions can expose them to vigilant prey[21] but may also create opportunities to exploit visibility—by improving their own detection of prey,[20,21] altering prey risk perception and hesitation,[18,28] or in some cases providing unexpected camouflage opportunities against the brightened night sky.[29]

The barn owl's striking color polymorphism offers a rare natural experiment[30] to test how conspicuous coloration functions in nocturnal predators exposed to fluctuating moonlight. Individuals range from reddish to pure white,[31–33] with paler morphs likely appearing more conspicuous under moonlight.[18] Why such coloration persists has sparked debate, and recent work has begun to unravel the genomic architecture and evolutionary history of this polymorphism.[32,34] Two non-mutually exclusive behavioral hypotheses have been proposed to explain how white plumage may shape predator-prey interactions under moonlight. The startle hypothesis posits that moonlight reflected off white plumage triggers prolonged freezing responses in rodents, thereby increasing capture opportunities.[18] By contrast, the camouflage hypothesis suggests that pale plumage achieves background matching against the brightened night sky, reducing detection by prey.[29] These hypotheses make distinct predictions about how white morphs should behave on moonlit nights, yet direct behavioral evidence from free-ranging individuals has so far been missing.

Here, we combine high-resolution biologging with lunar lightscape modeling to test these competing, non-mutually exclusive

This is an open access article under the CC BY license (http://creativecommons.org/licenses/by/4.0/).

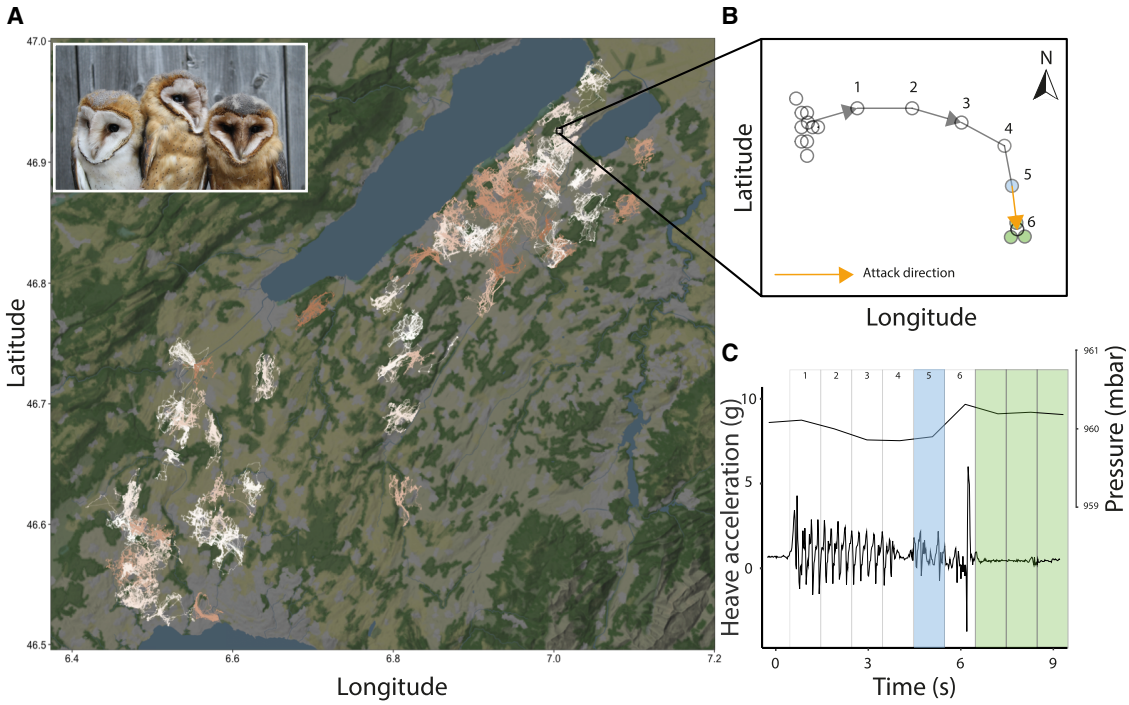


Figure 1. Multisensor biologging reveals the attack direction of hunting barn owls

This figure illustrates the study area, color polymorphism, and method used to reconstruct attack trajectories from GPS, accelerometry, and pressure data.

(A) Map of the study area showing the movement trajectories from 69 male barn owls, recorded during 78 individual tracking sessions across 2019 and 2020. Trajectories are color coded by individual plumage mean coloration score, ranging from reddish (score = 1) to pure white (score = 8), as shown in the top-left reference image. See also Figure S1.

(B) Example of a single hunting trajectory reconstructed from GPS fixes, with the attack direction (orange arrow) defined as the bearing between the descent onset (blue point) and the median position of the post-strike pause (green points).

(C) Corresponding time series of heave acceleration and pressure data from the same event, used to detect the characteristic vertical motion and altitude drop that mark the moment of strike. This integrated approach combines spatial and behavioral data to estimate the direction of each hunting attempt with high temporal and positional precision.

Image of barn owls in (A) courtesy of J. Bierer.

behavioral hypotheses in free-ranging barn owls. By tracking the movements of 69 breeding males over 354 nights and analyzing more than 17,600 hunting attempts during chick provisioning (Figure 1), we ask whether (1) the position and light intensity of the Moon influences attack directions relative to the Moon, (2) owls adjust their exposure to light by selecting specific periods of the night and moonlit versus shadowed microhabitats, and (3) such adjustments translate into differences in foraging effort, hunting success, and provisioning performance between color morphs. These analyses aim to clarify how coloration, behavioral plasticity, and environmental light interact to shape moonlight-dependent hunting strategies and to place the white-red polymorphism of barn owls in the broader context of light-mediated predator-prey interactions.

RESULTS AND DISCUSSION

White morphs align attacks to increase moonlight exposure

According to the startle hypothesis, white barn owls are expected to orient their attacks toward prey so that their ventral surface faces the Moon, using lunar light reflected off their plumage to increase visual exposure and trigger freezing responses in prey.[18] By contrast, a pure camouflage scenario based on background matching predicts that pale owls should preferentially use approach directions and light conditions that keep their ventral radiance close to that of the surrounding moonlit sky from the prey's viewpoint, so a camouflaging predator needs not systematically face the Moon but should instead select any approach path that maintains low predator-sky contrast.[3,29]

We first used circular statistics to describe how barn owls' attack directions are distributed relative to the Moon's position under different illumination levels. To maximize contrast while retaining sufficient sample sizes, we focused on 20 red males (color scores 1–4.6) and 20 white males (scores 7.5–8), corresponding to the lower and upper quartiles of the continuous scale, respectively. Plumage coloration was treated as a continuous variable across its full range (scores 1–8) in all subsequent statistical models (see STAR Methods). For each hunting event, we reconstructed the attack direction from the descent initiation point to the prey location and associated it with the Moon's azimuth and elevation at that time. Lunar illumination was estimated using a high-precision astronomical model[19] and categorized into three levels based on the empirical distribution of illumination values for descriptive purposes: no moonlight (Moon below the

CellPress
OPEN ACCESS

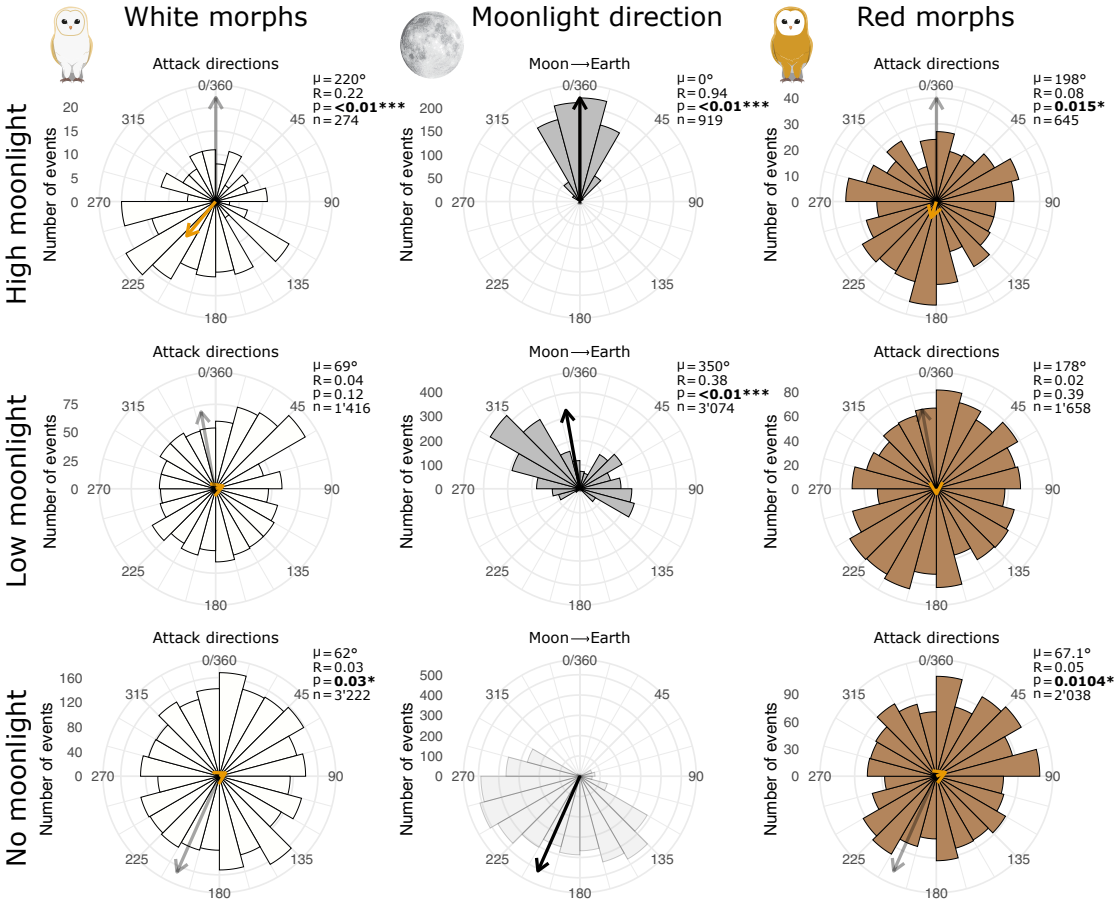


Figure 2. Attack orientations of white and red barn owls under different moonlight conditions

Circular histograms show the distribution of attack directions for the two extreme color morphs (white plumage score 7.5–8, left column; red score 1–4.6, right column) and the distribution of lunar azimuths at the time of each attack (central column). Lunar azimuth refers here to the direction of moonlight propagation at ground level, from the Moon toward the Earth's surface. Data are shown for three moonlight conditions: high moonlight (illumination index > 0.09; max = 0.202), low moonlight (0–0.09), and no moonlight (Moon below the horizon). Orange arrows indicate the mean attack direction (μ), while black arrows indicate the mean lunar azimuth. Arrow length is proportional to directional clustering (mean resultant length, R). For visual comparison across panels, the mean lunar azimuth is additionally shown as a semi-transparent arrow in all plots (transparent when the Moon is below the horizon). Sample sizes, mean directions, R values, and Rayleigh test statistics (α = 0.05) are provided within each panel.

horizon), low moonlight (illumination 0–0.09), and high moonlight (>0.09; maximum ≈0.20; see STAR Methods and Figure 1). Under high moonlight, both morphs showed non-uniform attack directions but differed in the strength of orientation. White males exhibited a clear preferred direction (μ = 220°) with a relatively long mean vector (R = 0.22, $p < 0.01$), whereas red males showed a similar mean angle but a shorter vector (R = 0.08, $p = 0.015$; Figure 2). During these same events, the incoming moonlight vector had a mean direction of μ = 0° (R = 0.94, $p < 0.01$), indicating that attacks were generally oriented toward the Moon (Figure 2). Under low or no moonlight, attack directions were much closer to uniform, and Rayleigh tests indicated weak or no orientation for both morphs ($p > 0.01$ in all cases; Figure 2).[35] Together, these circular analyses indicate that under high moonlight, both morphs show directional bias toward the Moon, but that clustering is stronger in white than in red males.

We then used a mixed-effects model of the moonlight alignment vector (MAV) to quantify continuously how the strength of this alignment varies with lunar illumination and plumage coloration. We quantified an MAV for each hunting attempt (Figure 3A). MAV is defined as the scalar projection of the moonlight vector (given by lunar azimuth and elevation, scaled by estimated intensity) onto the owl's attack vector (Equation 1). Positive MAV values indicate alignment (lunar light projected along the attack trajectory toward the prey), while negative values indicate divergence (attacks oriented away from the Moon). We modeled MAV using a generalized additive mixed model (GAMM), including moonlight intensity and plumage coloration. Because residual variance increased with moonlight intensity, we applied observation-level weights derived from a preliminary generalized least squares (GLS) model to reduce heteroscedasticity (see STAR Methods). The GAMM revealed a strong interaction between moonlight intensity and coloration (estimated degrees of freedom [EDF] ≈ 3.4, F = 23.21, $p < 0.001$; Table S1; N = 7,704 attacks from 69 individuals): MAV increased steeply with moonlight intensity in white owls, indicating that they progressively oriented their attacks to be more strongly aligned with the moonlight vector as nights grew brighter (Figure 3B).

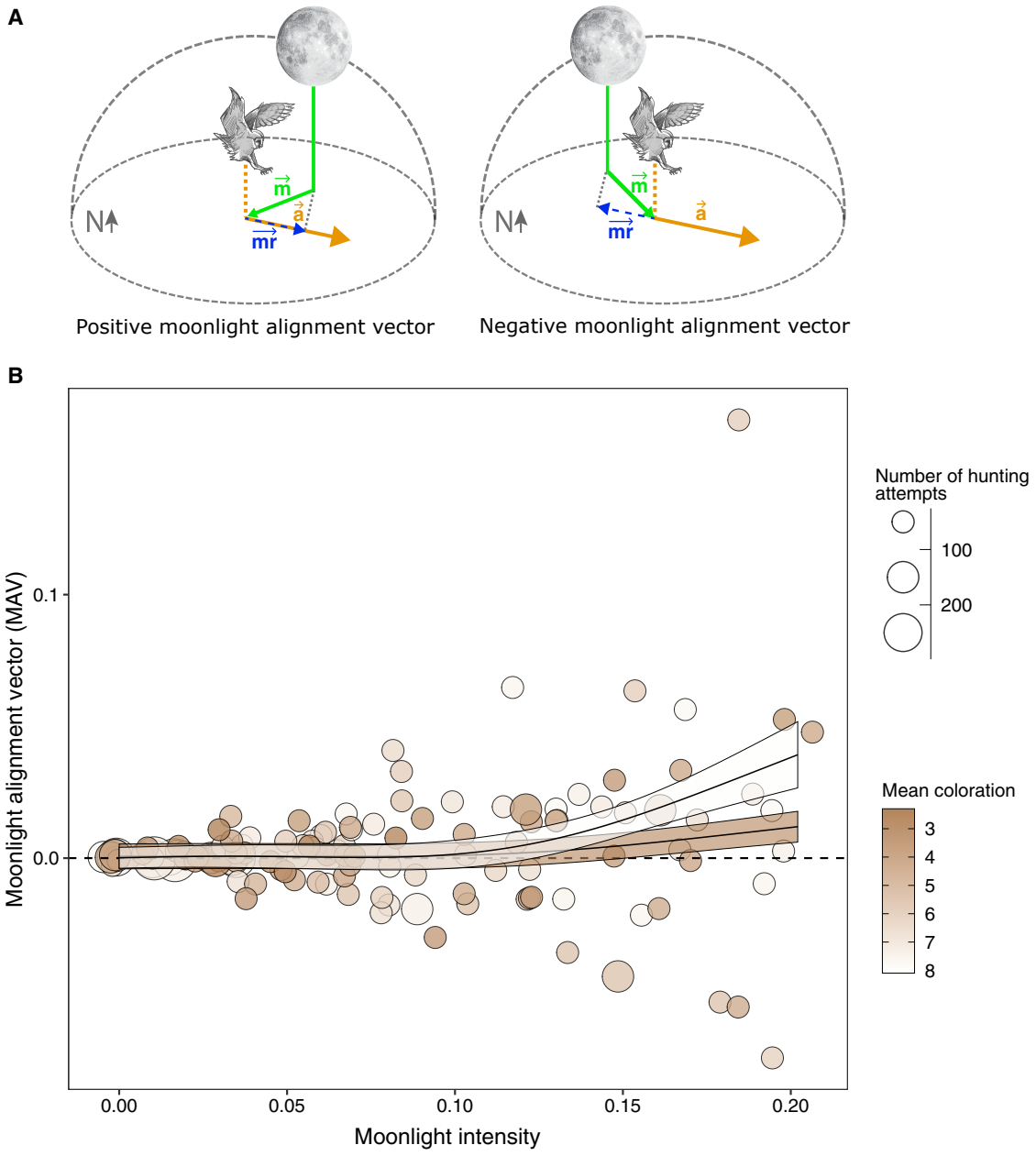


Figure 3. White morphs align attacks to increase moonlight exposure

(A) Conceptual diagram illustrating how the orientation of an owl's attack vector ($\vec{a}$, orange) relative to the incoming moonlight direction ($\vec{m}$, green) determines the projected moonlight alignment vector (MAV; $\overrightarrow{mr}$, blue). MAV is defined as the component of moonlight intensity projected along the owl's attack direction. MAV is a geometric index of alignment between attack direction and moonlight direction and does not represent measured reflectance or luminance. When the owl flies toward the Moon, moonlight is projected toward the prey (positive MAV). When flying away, light is diverted in the opposite direction (negative MAV).

(B) Relationship between ambient moonlight intensity and MAV (GAMM, n = 7,704 hunting attempts across 78 tracks from 69 individuals). See also Table S1. The vertical axis shows MAV values. Each point represents an individual-level mean MAV value within one of six equal-width bins of moonlight intensity. Dot size scales with the number of hunting attempts per bin, and color reflects mean plumage coloration (darker = redder). Plumage coloration is treated as a continuous variable throughout the analyses, and numeric labels shown on the color scale (1–8) are reference values along a continuous gradient and are not used as discrete categories. Curves represent smoothed trends for representative red and white morphs, and shaded ribbons indicate 95% CIs. Slight jitter is added for visibility. Owl illustrations in (A) by L. Willenegger.

In red males, MAV values remained weakly positive and varied little with illumination, consistent with a modest tendency to face the brightest part of the sky but without the pronounced strengthening seen in white males.

These MAV results indicate that white morphs increasingly adopt attack orientations that maximize projected ventral exposure to lunar illumination under bright conditions, in line with predictions derived from the startle hypothesis.[18] By contrast, a

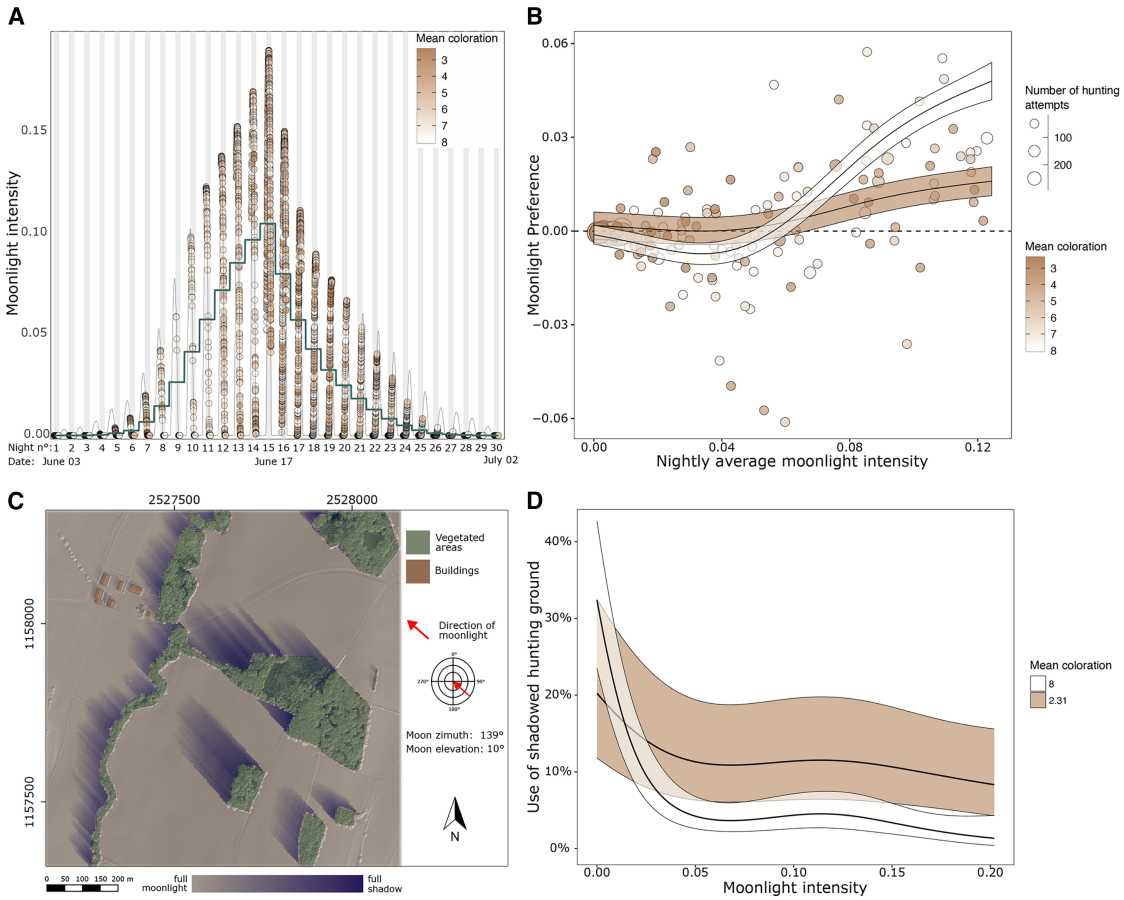


Figure 4. White morphs flexibly modulate spatiotemporal moonlight exposure

Barn owls adjust their foraging behavior across the lunar cycle, within nights, and across moonlit landscapes in relation to plumage coloration. Plumage coloration is treated as a continuous variable throughout the analyses, and numeric labels shown on the color scale (1–8) are reference values along a continuous gradient and are not used as discrete categories.

(A) Timing of 6,039 hunting events by 29 male barn owls across one lunar month (3 June–2 July). The black line shows the change in moonlight intensity throughout each night, and the dark green bar shows nightly means. Gray shading denotes night time, and white areas indicate daytime. Circles represent individual hunting events, color coded by owl plumage (reddish to white), illustrating the timing and illumination conditions of attacks. See also Figure S1.

(B) Moonlight preference was modeled as the deviation between moonlight intensity at each attack and the nightly mean moonlight illumination (GAMM; n = 17,039 attacks across 78 tracks from 69 individuals). See also Table S2. Positive values indicate selection for brighter-than-average periods. Dots show individual means across 12 moonlight bins, scaled by the number of attempts. Dot size scales with the number of hunting attempts per bin. Slight jitter is added for visibility.

(C) Example of modeled moonlight exposure, based on lunar position (azimuth 139°, elevation 10°). Illumination levels were estimated from local terrain and obstacle height (vegetation in green, buildings in brown) and rendered at 5 m × 5 m resolution, and dark areas indicate full shadow.

(D) Probability of hunting in shadowed ground, modeled across moonlight intensities (GAMM; n = 7,348 attacks across 76 tracks from 67 individuals). See also Table S3. Solid lines show predictions for representative white (score = 8) and red (score = 2.3) morphs, and shaded ribbons represent 95% CIs.

pure background-matching scenario would not predict such a systematic increase in Moon-facing alignment with increasing illumination.[3,29,36–38]

White morphs flexibly modulate spatiotemporal moonlight exposure

If white morphs adjust attack orientation to increase alignment with the Moon, do they also adjust when and where they hunt to exploit the brightest parts of the night? We addressed this by examining (1) within-night temporal selection for particular illumination levels and (2) spatial use of moonlit versus shadowed areas across the lightscape (Figure 4). Lunar cycles and the Moon's apparent motion generate predictable but dynamic shifts in nocturnal illumination,[19,20] while local structures such as trees, buildings, and terrain create fine-scale patchiness in the distribution of light and shadow.

For each hunting attempt, we quantified temporal moonlight preference as the difference between moonlight intensity at each hunting event and the mean moonlight intensity available during that individual's active hunting period that night (see STAR Methods; Figure 4A). Negative values indicate that the owl hunted during darker-than-average intervals, whereas positive values indicate selection for brighter-than-average intervals relative to the temporal light environment it experienced.[19] This measure captures individual selection for particular time windows of illumination, rather than selection on absolute moonlight levels (Figure 4A; see STAR Methods). A weighted GAMM revealed that temporal moonlight preference depended strongly

on both moonlight intensity and plumage coloration (Table S2). During bright nights, white males concentrated their hunting activity during the brightest intervals of their active period, whereas during dim nights they tended to avoid relatively brighter periods (Figure 4B; Table S2). This pattern indicates flexible timing: white morphs exploit strongly illuminated windows when moonlight is high but avoid marginally illuminated periods when moonlight is low and conspicuousness may not be offset by a strong behavioral effect on prey. By contrast, red males showed only a modest and more monotonic tendency to hunt during intervals slightly brighter than their nightly average (Figure 4B), a pattern consistent with taking advantage of improved visibility rather than actively amplifying visual exposure.[20,23,39]

We then asked whether barn owls similarly fine-tune where they hunt in relation to local illumination. By combining high-resolution topography, vegetation, and building data with the moonlight model, we generated shadow maps at 5 m × 5 m resolution around each hunting event and classified each attempt as occurring in direct moonlight or in shadow (Figure 4C). A binomial GAMM showed that the probability of hunting in shadowed ground decreased with increasing moonlight intensity and that this decrease was more pronounced in white males than in red males (Figure 4D; Table S3). White morphs reduced the proportion of hunting attempts in shadow from ∼30% under low illumination to ∼5% under high moonlight, while red morphs showed a more moderate decline (from ∼20% to ∼10%). Hunting strategy also influenced microhabitat choice, with perching ("sit-and-wait") hunts occurring more frequently in shadow than aerial hunts, independent of plumage coloration and moonlight intensity (Table S3).

Together, these temporal and spatial adjustments reveal a coordinated strategy in white barn owls: they time and place their hunts to maximize ventral exposure to strong moonlight when it is available, while avoiding periods and areas where their conspicuous plumage would be exposed (e.g., sit-and-wait hunts) or only weakly illuminated. Red morphs, by contrast, show a more limited shift toward brighter periods and open areas, consistent with a general benefit of better visibility but not with actively amplifying conspicuousness.[20,21]

Few nocturnal predators and prey adjust microhabitat selection so strongly in response to moonlight, and when they do, it is typically to reduce predation risk or improve their own detection abilities rather than to increase their detectability to others.[20,21] In many rodent species, for example, moonlight reduces activity and drives individuals into cover to avoid detection and predation.[20,21] This contrast strengthens our interpretation that barn owls are not merely tracking prey distribution but instead that white morphs actively select bright patches in space and time to enhance the functional impact of their bright plumage on prey.[18,20,36,37]

White morphs achieve higher capture rates and shorter hunts under bright moonlight

The behavioral adjustments described above raise a key question: do these strategies translate into foraging performance differences between morphs? To address this, we modeled three complementary metrics across color morphs and moonlight levels: (1) per-attack hunting success (capture probability), (2) prey capture rate (capture per hour of active hunting), and (3) nightly foraging duration (time between the first and last hunting attempt).

At the attack level, a binomial generalized linear mixed model (GLMM) revealed no strong evidence that capture probability changed with moonlight intensity, plumage coloration, and their interaction (odds ratio for moonlight × color = 1.02, 95% confidence interval [CI] = 0.98–1.08, p = 0.318; Table S4). Capture probability also did not differ between attacks occurring under direct moonlight, in shadowed areas, or in the absence of moonlight, and these effects did not interact with plumage coloration (Table S4). Pairwise contrasts revealed that, within white morphs, per-attack success was similar across light environments: capture probability did not differ between attacks performed under no moonlight and in shadowed areas (odds ratio = 0.85, p = 0.45), between no moonlight and moonlit areas (odds ratio = 0.91, p = 0.41), or between shadowed and moonlit areas (odds ratio = 1.07, p = 0.88). Likewise, red morphs showed no significant differences in per-attack success across moonlight availability categories (no Moon vs. shadow: odds ratio = 1.11, p = 0.86; no Moon vs. moonlit: odds ratio = 0.83, p = 0.30; shadow vs. moonlit: odds ratio = 0.75, p = 0.31). Thus, both white and red morphs maintained broadly similar and stable attack-level success across light environments.

By contrast, hunting strategy had an effect on capture probability. Sit-and-wait attacks were significantly more successful than aerial attacks on the wing (odds ratio = 1.29, 95% CI = 1.17–1.42, p < 0.001; Table S4). This pattern is consistent with previous results from the same population, where perching hunts were also shown to yield higher strike success than aerial attacks[17] and reflects intrinsic differences between hunting modes rather than light-dependent effects.

Together, these results indicate that neither moonlight nor plumage coloration directly affects the success of individual hunting strikes. Instead, when considered alongside the temporal and spatial behavioral adjustments described above, they suggest that white owls maintain stable per-attack success despite increased conspicuousness by flexibly adjusting when and where they hunt, thereby translating moonlight exposure into higher overall foraging efficiency rather than higher strike success per se. These results suggest that the primary effect of moonlight and coloration is not on the success of individual strikes but on how often and how efficiently owls can launch successful attacks over the night. Moonlight and coloration shape foraging performance indirectly—by altering attack orientation, timing, and spatial exposure—rather than by changing the probability that a given strike succeeds.

At the nightly scale, clear differences emerged between morphs (Figure 5). White males' prey capture rate increased markedly with mean nightly moonlight intensity and exceeded that of red males (GAMM: EDF = 3.93, F = 367.09, p < 0.001; Figure 5A; Table S5). At the same time, their nightly foraging duration decreased with increasing illumination, especially in bright nights where white morphs provisioned their broods in shorter time spans than red morphs (LMM interaction moonlight × color: estimate = 2.44, 95% CI = 0.62–4.27, p = 0.009; Figure 5B; Table S6). Red males showed little change in either capture rate or foraging duration across the moonlight gradient.

Because per-attack success was similar between morphs, the higher capture rate and shorter foraging time of white owls under

CellPress
OPEN ACCESS

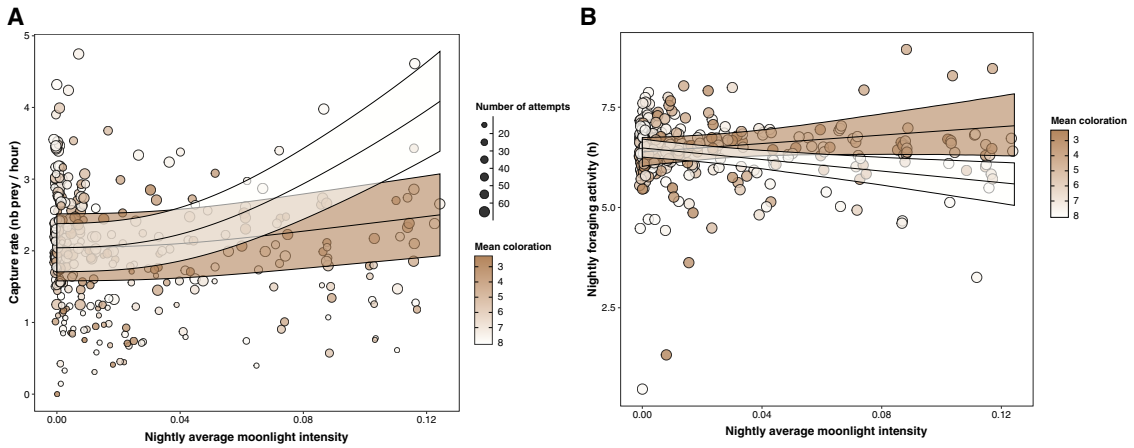


Figure 5. White morphs achieve higher capture rates and shorter hunts under bright moonlight

Prey capture rate and foraging duration in relation to varying lunar illumination in relation to their plumage coloration. Plumage coloration is treated as a continuous variable throughout the analyses, and numeric labels shown on the color scale (1–8) are reference values along a continuous gradient and are not used as discrete categories.

(A) Prey capture rate (number of prey items captured per hour of active hunting) as a function of nightly average moonlight intensity. Colored dots represent individual nightly capture rates, scaled by the number of hunting attempts per bin and color coded by plumage score (from reddish to white).

(B) Total foraging duration, defined as the time elapsed between the first and last hunting attempt of the night, shown in relation to moonlight intensity. In both panels, solid lines indicate model-predicted means for representative red (coloration score = 2.3) and white (score = 8) morphs, and shaded ribbons represent 95% CIs. Jitter was applied along the *x* axis to reduce point overlap. Analyses include 354 nights from 69 individuals and are based on GAMMs (A) and linear mixed models (B), respectively.

See also Tables S4–S6.

bright moonlight are best explained by an increased frequency and efficiency of encounters rather than by more accurate strikes once an attack is initiated. One plausible mechanism, consistent with previous experimental work, is that increased ventral exposure of white owls under strong moonlight could increase the likelihood of a hesitation response in prey, thereby extending the window of vulnerability and allowing owls to initiate more attacks per unit time.[18] Our field data do not test prey behavior directly, so this mechanistic interpretation remains inferential.

Importantly, these performance advantages arise within a relatively narrow temporal window. At our study site, illumination exceeding 50% of the maximum occurs during only ~4% of the lunar cycle (Figure 4A), concentrated in the few nights surrounding the full Moon. During these nights, however, high illumination can prevail for up to ~70% of the owls' active hunting period, creating a brief but substantial opportunity to maximize prey delivery. Given the high energetic demands of rapidly growing chicks,[40] failing to exploit these windows could reduce chick growth and survival. Previous work has shown that barn owls in this population time their breeding so that peak chick provisioning coincides with the brightest nights of the lunar cycle.[18] Our results clarify a key mechanistic link: during those same nights, white males achieve higher capture rates and shorter foraging bouts by dynamically adjusting attack orientation, microhabitat selection, and temporal activity.

Contextualizing moonlight-dependent foraging patterns

Similar light-dependent foraging patterns have been reported in other nocturnal or crepuscular predators. Visually oriented insectivores such as nightjars (*Caprimulgus europaeus*) increase foraging activity under bright moonlight and may even align breeding phenology with lunar cycles, presumably because brighter skies improve detection of flying prey and can coincide with higher insect availability.[20,41,42] These examples show that exploiting bright moonlight is not unique to barn owls. What distinguishes our system is that white males combine this general benefit of illumination with a coordinated suite of behaviors—orienting attacks toward the Moon and preferentially using exposed microhabitats—that modulate how their conspicuous plumage is presented to prey. Thus, while the underlying mechanisms may differ among taxa, our results together with those from nightjars suggest that lunar lightscapes may represent a widespread but under-recognized axis of ecological and evolutionary differentiation among nocturnal predators.

Our findings also help reconcile discrepancies with an earlier GPS-based study that reported reduced hunting success in red morphs under bright moonlight. In San-Jose et al.,[18] hunting attempts were inferred indirectly from GPS movement patterns and considered successful only if followed by a return to the nest, which may have underestimated the true number of attempts—particularly those made from perches—and may have classified some nest visits without prey as successful. By contrast, our multisensor biologging approach provides high-resolution data that detect individual hunting attempts and their outcome with high precision.[17,43]

Our analysis has important limitations regarding realized nocturnal illumination. Specifically, our moonlight estimates quantify the lunar component of the lightscape from astronomical geometry, topography, and obstacles under clear-sky assumptions; they are not direct measurements of the total light environment experienced at each hunting event. We lacked time-resolved data on cloud cover, atmospheric turbidity, fine-scale surface reflectance, and spatially explicit artificial lighting, all of which can modify ground-level illumination. These unmeasured

factors are therefore expected to add variance to the illumination gradient and reduce precision. They would bias the inference only if they were systematically confounded with plumage color or sampling time, rather than varying across individuals and nights more generally. However, this does not appear to be the case in our study, as shown by the distribution of tracking sessions across individuals, plumage coloration, and lunar conditions (Figure S1; see also Figure 4A). Second, although artificial light at night can strongly modify sky brightness and interacts with cloud cover in urbanized landscapes,[44] we did not have spatially explicit data on the intensity, spectrum, and timing of artificial light sources across our study area. Our sites are embedded in a predominantly agricultural matrix with relatively low levels of direct lighting, but any unaccounted artificial light is again likely to add noise around our mechanistic moonlight index rather than to create the consistent, morph-specific patterns we report. Taken together, these limitations suggest that our estimates of morph differences in alignment and foraging performance under bright conditions are conservative and may understate, rather than exaggerate, the behavioral responses of barn owls to natural lunar lightscapes.

Lunar lightscapes may act as a driver of conspicuous hunting strategies and color variation

Together, these findings show that conspicuous coloration in barn owls confers substantial foraging advantages under moonlit conditions when combined with flexible behavior. White morphs do not remain static in their exposure. Instead, they flexibly adjust their behavior in several coordinated ways: during bright nights, they orient their attacks facing the Moon, thereby maximizing lunar illumination reflected off their ventral plumage; they time their hunting activity to coincide with the brightest periods of the night; and they preferentially select exposed microhabitats rather than shadowed areas. These strategies collectively increase their conspicuousness to prey and allow white morphs to achieve higher capture rates and shorter foraging bouts without reducing per-attack success. Crucially, this advantage is restricted to a narrow set of conditions—bright, moonlit nights during breeding—and the same conspicuousness is likely to be costly when illumination is low, cloud cover is high, or predators themselves face increased predation risk. By contrast, red morphs maintain more cryptic strategies, showing only slight adjustments in timing or habitat use and no consistent orientation toward the Moon. As a result, red morphs maintain stable hunting success across the lunar cycle but achieve lower overall efficiency during bright conditions. This constellation of behaviors is more consistent with a startle-based interpretation than with a pure background-matching scenario. More specifically, our field data show that white and red morphs differ systematically in attack alignment, temporal use of bright periods, microhabitat exposure, and nightly foraging performance under moonlight. These behavioral patterns are compatible with a startle-based mechanism previously demonstrated experimentally, but they do not by themselves constitute direct evidence of prey perception or prey freezing in the wild.[3–5,18,29,45–47]

This study provides evidence consistent with the idea that startle-like displays can function as an offensive hunting tactic in predators rather than solely as an antipredator defense[4,45–47]—a striking reversal of their classical role. While previous work demonstrated experimentally that white plumage triggers prey freezing and suggested this mechanism could improve hunting success,[18] our findings show that white and red barn owls differ systematically in how they align their attacks with the Moon, use illuminated microhabitats, and adjust foraging schedules, and that white males gain a foraging efficiency advantage under bright moonlight. These patterns are compatible with a startle-based mechanism operating in free-ranging predators, even though we did not measure prey behavior directly. The ability of white barn owls to dynamically exploit moonlight illustrates behavioral plasticity as a key evolutionary strategy, allowing them to balance the trade-offs between conspicuousness and stealth. Although earlier studies have shown that bright plumage in nocturnal species can facilitate mate attraction[27] or intraspecific signaling,[26] intensively reflective white plumage has evolved repeatedly in both predators and prey inhabiting dim-light environments.[41,48–51] Our results raise the possibility that such traits do not merely enhance visibility but also shape detection, hesitation, and other interactions under moonlit conditions—offering a new framework for understanding conspicuousness in the dark.[1,2,14]

Finally, the finding that white morphs capitalize on brief windows of intense illumination, while red morphs remain consistently cryptic, highlights how lunar lightscapes can create fluctuating selection pressures that help maintain stable color polymorphisms. In barn owls, the prevalence of white color in males[52]—who invest more in provisioning than females[17,53]—and the genomic architecture and spatial dynamics of the white-red continuum[14,32–34] suggest that moonlight-driven advantages in prey capture could contribute to this sex-biased coloration. At the same time, recent genomic work shows that the color polymorphism is oligogenic and embedded in a heterogeneous selection landscape, with color-associated alleles responding to climatic, demographic, and density-dependent forces across space and time.[32,34] Together with evidence that melanin-based traits in this species covary with physiology,[54] life history,[55,56] and dispersal,[57] this implies that red morphs are likely favored under alternative ecological conditions so that neither morph is universally superior. More broadly, our work underscores the potential for nocturnal lightscapes to shape the evolution of animal coloration in largely unexplored ways.[1,2,14] As artificial lighting increasingly transforms natural nightscapes,[44] understanding how species evolved under lunar cycles becomes critical. Disruption of these ancient rhythms could reshape ecological interactions and erode evolutionary processes finely tuned to the cadence of moonlight over millennia.[20,21,23,24,44]

RESOURCE AVAILABILITY

Lead contact

Requests for further information and resources should be directed to and will be fulfilled by the lead contact, Kim Schalcher (kim.schalcher@icloud.com).

Materials availability

This study did not generate any new, unique reagents.

Data and code availability

- The data curated for this study have been deposited at Mendeley Data and are publicly available at 10.17632/tvnpvhf2yj.2 as of the date of publication.

- All original code has been deposited at Mendeley Data and is publicly available at 10.17632/tvnpvhf2yj.2 as of the date of publication.
- Any additional information required to reanalyze the data reported in this paper is available from the lead contact upon request.

Received: November 1, 2025
Revised: January 30, 2026
Accepted: May 11, 2026
Published: June 8, 2026

ACKNOWLEDGMENTS

This study was funded by the Swiss National Science Foundation (grant no. 31003A_173178). We thank Luis San-Jose Garcia for laying the conceptual foundation on which this project was built. We are also deeply grateful to Emily L.C. Shepard and Hannah H. Williams for their invaluable guidance in processing the biologging data and identifying behavioral signatures. We thank Kamran Safi for his feedback at the early stages of the project. We thank A.P. Machado, L. Ançay, N. Külling, A.-C. Heinz, M. Froehly, M. Calvani, N. Sironi, L. Legrand, D. Zurkinden, R. Allemand, and L. Hulaas for their dedicated assistance during fieldwork. Finally, we thank J. Bierer for providing the barn owl photograph and L. Willenegger for providing barn owl drawings. We thank Will Allen, Jolyon Troscianko, and two anonymous reviewers that helped improve this work substantially.

AUTHOR CONTRIBUTIONS

K.S., P.B., and A.R. conceptualized the study; K.S., E.M., R.S., R.B., B.A., and P.B. developed the methodology; K.S. developed the software; K.S. and P.B. performed the formal analysis; K.S., E.M., and P.B. carried out the investigation; K.S. curated the data; K.S., P.B., and A.R. wrote the original draft; K.S., E.M., R.S., R.B., B.A., P.B., and A.R. reviewed and edited the manuscript; K.S. prepared the visualizations; P.B. and A.R. supervised the project; A.R. administered the project; and B.A. and A.R. acquired funding.

DECLARATION OF INTERESTS

The authors declare no competing interests.

DECLARATION OF GENERATIVE AI AND AI-ASSISTED TECHNOLOGIES IN THE WRITING PROCESS

During the preparation of this work, the authors used an AI-based language model (ChatGPT by OpenAI) in order to refine the text for conciseness to meet word count requirements. After using this tool or service, the authors reviewed and edited the content as needed and take full responsibility for the content of the publication.

STAR★METHODS

Detailed methods are provided in the online version of this paper and include the following:

- KEY RESOURCES TABLE
- EXPERIMENTAL MODEL AND STUDY PARTICIPANT DETAILS
  - Ethics Statement
  - Study Area and Tag Deployment
- METHOD DETAILS
  - Plumage coloration
  - Tag deployment
  - Camera trap validation
  - Data processing
- QUANTIFICATION AND STATISTICAL ANALYSIS
  - Statistical framework
  - Attack orientation
  - Alignment to moonlight vector
  - Spatiotemporal modulation of foraging exposure to moonlight
  - Foraging outcomes under moonlight: success, rate, and duration

SUPPLEMENTAL INFORMATION

Supplemental information can be found online at https://doi.org/10.1016/j.cub.2026.05.020.

REFERENCES

1. Cuthill, I.C., Allen, W.L., Arbuckle, K., Caspers, B., Chaplin, G., Hauber, M.E., Hill, G.E., Jablonski, N.G., Jiggins, C.D., Kelber, A., et al. (2017). The biology of color. Science *357*, eaan0221. https://doi.org/10.1126/science.aan0221.
2. Orteu, A., and Jiggins, C.D. (2020). The genomics of coloration provides insights into adaptive evolution. Nat. Rev. Genet. *21*, 461–475. https://doi.org/10.1038/s41576-020-0234-z.
3. Cuthill, I.C. (2019). Camouflage. J. Zool. *308*, 75–92. https://doi.org/10.1111/jzo.12682.
4. Umbers, K.D.L., Lehtonen, J., and Mappes, J. (2015). Deimatic displays. Curr. Biol. *25*, R58–R59. https://doi.org/10.1016/j.cub.2014.11.011.
5. Ruxton, G.D., Allen, W.L., Sherratt, T.N., and Speed, M.P. (2019). Avoiding Attack: the Evolutionary Ecology of Crypsis, Aposematism, and Mimicry (Oxford University Press). https://doi.org/10.1093/oso/9780199688678.001.0001.
6. Stuart-Fox, D., and Moussalli, A. (2009). Camouflage, communication and thermoregulation: Lessons from colour changing organisms. Philos. Trans. R. Soc. B *364*, 463–470. https://doi.org/10.1098/rstb.2008.0254.
7. Théry, M., and Casas, J. (2002). Predator and prey views of spider camouflage. Nature *415*, 133. https://doi.org/10.1038/415133a.
8. Caro, T., Izzo, A., Reiner, R.C., Walker, H., and Stankowich, T. (2014). The function of zebra stripes. Nat. Commun. *5*, 3535. https://doi.org/10.1038/ncomms4535.
9. Bond, A.B., and Kamil, A.C. (2002). Visual predators select for crypticity and polymorphism in virtual prey. Nature *415*, 609–613. https://doi.org/10.1038/415609a.
10. Losey, J.E., Harmon, J., Ballantyne, F., and Brown, C. (1997). A polymorphism maintained by opposite patterns of parasitism and predation. Nature *388*, 269–272. https://doi.org/10.1038/40849.
11. Pembury Smith, M.Q.R., and Ruxton, G.D. (2020). Camouflage in predators. Biol. Rev. *95*, 1325–1340. https://doi.org/10.1111/brv.12612.
12. Chuang, C.-Y., Yang, E.-C., and Tso, I.-M. (2007). Diurnal and nocturnal prey luring of a colorful predator. J. Exp. Biol. *210*, 3830–3837. https://doi.org/10.1242/jeb.007328.
13. Blamires, S.J., Hou, C., Chen, L.-F., Liao, C.-P., and Tso, I.-M. (2014). A predator's body coloration enhances its foraging profitability by day and night. Behav. Ecol. Sociobiol. *68*, 1253–1260. https://doi.org/10.1007/s00265-014-1736-5.
14. Roulin, A. (2004). The evolution, maintenance and adaptive function of genetic colour polymorphism in birds. Biol. Rev. *79*, 815–848. https://doi.org/10.1017/S1464793104006487.
15. Clark, C.J., LePiane, K., and Liu, L. (2020). Evolution and ecology of silent flight in owls and other flying vertebrates. Integr. Organ. Biol. *2*, obaa001. https://doi.org/10.1093/iob/obaa001.
16. Bachmann, T., Mühlenbruch, G., and Wagner, H. (2011). The barn owl wing: An inspiration for silent flight in the aviation industry? Proc. SPIE *7975*, 142–155. https://doi.org/10.1117/12.882703.
17. Schalcher, K., Milliet, E., Séchaud, R., Bühler, R., Almasi, B., Potier, S., Becciu, P., Roulin, A., and Shepard, E.L.C. (2024). Landing force reveals new form of motion-induced sound camouflage in a wild predator. eLife *12*, e87775. https://doi.org/10.7554/eLife.87775.
18. San-Jose, L.M., Séchaud, R., Schalcher, K., Judes, C., Questiaux, A., Oliveira-Xavier, A., Gémard, C., Almasi, B., Béziers, P., Kelber, A., et al. (2019). Differential fitness effects of moonlight on plumage colour morphs in barn owls. Nat. Ecol. Evol. *3*, 1331–1340. https://doi.org/10.1038/s41559-019-0967-2.

19. Śmielak, M.K. (2023). Biologically meaningful moonlight measures and their application in ecological research. Behav. Ecol. Sociobiol. *77*, 21. https://doi.org/10.1007/s00265-022-03287-2.

20. Kronfeld-Schor, N., Dominoni, D., de la Iglesia, H., Levy, O., Herzog, E.D., Dayan, T., and Helfrich-Forster, C. (2013). Chronobiology by moonlight. Proc. R. Soc. B. *280*, 20123088. https://doi.org/10.1098/rspb.2012.3088.

21. Prugh, L.R., and Golden, C.D. (2014). Does moonlight increase predation risk? Meta-analysis reveals divergent responses of nocturnal mammals to lunar cycles. J. Anim. Ecol. *83*, 504–514. https://doi.org/10.1111/1365-2656.12148.

22. Hanlon, R.T., Naud, M.J., Forsythe, J.W., Hall, K., Watson, A.C., and McKechnie, J. (2007). Adaptable night camouflage by cuttlefish. Am. Nat. *169*, 543–551. https://doi.org/10.1086/512106.

23. Warrant, E.J. (2007). Visual ecology: Hiding in the dark. Curr. Biol. *17*, R209–R211. https://doi.org/10.1016/j.cub.2007.01.043.

24. Dacke, M., Nilsson, D.-E., Scholtz, C.H., Byrne, M., and Warrant, E.J. (2003). Insect orientation to polarized moonlight. Nature *424*, 33. https://doi.org/10.1038/424033a.

25. Dickerson, A.L., Hall, M.L., and Jones, T.M. (2023). Effects of variation in natural and artificial light at night on acoustic communication: A review and prospectus. Anim. Behav. *198*, 93–105. https://doi.org/10.1016/j.anbehav.2023.01.018.

26. Penteriani, V., and Delgado, M. del M. (2017). Living in the dark does not mean a blind life: Bird and mammal visual communication in dim light. Phil. Trans. R. Soc. B *372*, 20160064. https://doi.org/10.1098/rstb.2016.0064.

27. Penteriani, V., Delgado, M. del M., Campioni, L., and Lourenço, R. (2010). Moonlight makes owls more chatty. PLoS One *5*, e8696. https://doi.org/10.1371/journal.pone.0008696.

28. Woo, T., Liang, X., Evans, D.A., Fernandez, O., Kretschmer, F., Reiter, S., and Laurent, G. (2023). The dynamics of pattern matching in camouflaging cuttlefish. Nature *619*, 122–128. https://doi.org/10.1038/s41586-023-06259-2.

29. Negro, J.J., Bará, S., Galadí-Enríquez, D., Nieves, J.L., Martínez-Domingo, M.A., Ferrero, A., Campos, J., Bao-Varela, C., Masana, E., and Camacho, C. (2025). Nocturnal camouflage through background matching against moonlight. Proc. Natl. Acad. Sci. USA *122*, e2406808121. https://doi.org/10.1073/pnas.2406808121.

30. Delgado, M. del M., Penteriani, V., Revilla, E., and Nams, V.O. (2010). The effect of phenotypic traits and external cues on natal dispersal movements. J. Anim. Ecol. *79*, 620–632. https://doi.org/10.1111/j.1365-2656.2009.01655.x.

31. Roulin, A. (2020). Barn Owls: Evolution and Ecology (Cambridge University Press). https://doi.org/10.1017/9781316694114.

32. Cumer, T., Machado, A.P., San-Jose, L.M., Ducrest, A.-L., Simon, C., Roulin, A., and Goudet, J. (2024). The genomic architecture of continuous plumage colour variation in the European barn owl (Tyto alba). Proc. R. Soc. B. *291*, 20231995. https://doi.org/10.1098/rspb.2023.1995.

33. Antoniazza, S., Kanitz, R., Neuenschwander, S., Burri, R., Gaigher, A., Roulin, A., and Goudet, J. (2014). Natural selection in a postglacial range expansion: the case of the colour cline in the European barn owl. Mol. Ecol. *23*, 5508–5523. https://doi.org/10.1111/mec.12957.

34. Cumer, T., Topaloudis, A., Lavanchy, E., Ducrest, A.-L., Cabello, S.S., Hewett, A., Becciu, P., Simon, C., Almasi, B., Roulin, A., et al. (2025). Genomic bases of short-term evolution in the wild revealed by long-term monitoring and population-scale sequencing. Preprint at bioRxiv. https://doi.org/10.1101/2025.10.01.679793.

35. Landler, L., Ruxton, G.D., and Malkemper, E.P. (2020). Grouped circular data in biology: advice for effectively implementing statistical procedures. Behav. Ecol. Sociobiol. *74*, 100. https://doi.org/10.1007/s00265-020-02881-6.

36. Roberts, A. (1978). Pineal eye and behaviour in Xenopus tadpoles. Nature *273*, 774–775. https://doi.org/10.1038/273774a0.

37. Yoshizawa, M., and Jeffery, W.R. (2008). Shadow response in the blind cavefish Astyanax reveals conservation of a functional pineal eye. J. Exp. Biol. *211*, 292–299. https://doi.org/10.1242/jeb.012864.

38. Donohue, C.G., Hemmi, J.M., and Kelley, J.L. (2020). Countershading enhances camouflage by reducing prey contrast. Proc. R. Soc. B. *287*, 20200477. https://doi.org/10.1098/rspb.2020.0477.

39. Orlowski, J., Harmening, W., and Wagner, H. (2012). Night vision in barn owls: visual acuity and contrast sensitivity under dark adaptation. J. Vis. *12*, 4. https://doi.org/10.1167/12.13.4.

40. Roulin, A., Ducrest, A.L., and Dijkstra, C. (1999). Effect of brood size manipulations on parents and offspring in the barn owl Tyto alba. Ardea *87*, 91–100.

41. Brigham, R.M., Ng, J., Poulin, R.G., and Grindal, S.D. (2011). Common nighthawk (Chordeiles minor). In The Birds of North America (Cornell Laboratory of Ornithology).

42. Norevik, G., Åkesson, S., Andersson, A., Bäckman, J., and Hedenström, A. (2019). The lunar cycle drives migration of a nocturnal bird. PLoS Biol. *17*, e3000456. https://doi.org/10.1371/journal.pbio.3000456.

43. Wilson, R.P., Holton, M.D., di Virgilio, A., Williams, H., Shepard, E.L.C., Lambertucci, S., Quintana, F., Sala, J.E., Balaji, B., Lee, E.S., et al. (2018). Give the machine a hand: a Boolean time-based decision-tree template for rapidly finding animal behaviours in multisensor data. Methods Ecol. Evol. *9*, 2206–2215. https://doi.org/10.1111/2041-210X.13069.

44. Kyba, C.C.M., Altıntaş, Y.Ö., Walker, C.E., and Newhouse, M. (2023). Citizen scientists report global rapid reductions in the visibility of stars from 2011 to 2022. Science *379*, 265–268. https://doi.org/10.1126/science.abq7781.

45. Umbers, K.D.L., De Bona, S., White, T.E., Lehtonen, J., Mappes, J., and Endler, J.A. (2017). Deimatism: a neglected component of antipredator defence. Biol. Lett. *13*, 20160936. https://doi.org/10.1098/rsbl.2016.0936.

46. Drinkwater, E., Allen, W.L., Endler, J.A., Hanlon, R.T., Holmes, G., Homziak, N.T., Kang, C., Leavell, B.C., Lehtonen, J., Loeffler-Henry, K., et al. (2022). A synthesis of deimatic behaviour. Biol. Rev. *97*, 2237–2267. https://doi.org/10.1111/brv.12891.

47. Umbers, K.D.L., and Mappes, J. (2016). Towards a tractable working hypothesis for deimatic displays. Anim. Behav. *113*, e5–e7. https://doi.org/10.1016/j.anbehav.2016.01.002.

48. Dunning, J., Patil, A., D'Alba, L., Bond, A.L., Debruyn, G., Dhinojwala, A., Shawkey, M., and Jenni, L. (2023). How woodcocks produce the most brilliant white plumage patches among the birds. J. R. Soc. Interface. *20*, 20220920. https://doi.org/10.1098/rsif.2022.0920.

49. Tickell, W.L.N. (2003). White plumage. Waterbirds *26*, 1–12. https://doi.org/10.1675/1524-4695(2003)026[0001:WP]2.0.CO;2.

50. Stoddard, M.C., and Prum, R.O. (2011). How colorful are birds? Evolution of the avian plumage color gamut. Behav. Ecol. *22*, 1042–1052. https://doi.org/10.1093/beheco/arr088.

51. Camacho, C., Sáez-Gómez, P., Hidalgo-Rodríguez, P., Rabadán-González, J., Molina, C., and Negro, J.J. (2022). Leucistic plumage as a result of progressive greying in a cryptic nocturnal bird. Sci. Rep. *12*, 3411. https://doi.org/10.1038/s41598-022-07360-8.

52. Roulin, A., and Jensen, H. (2015). Sex-linked inheritance, genetic correlations and sexual dimorphism in three melanin-based colour traits in the barn owl. J. Evol. Biol. *28*, 655–666. https://doi.org/10.1111/jeb.12596.

53. Becciu, P., Schalcher, K., Milliet, E., Savage, J.L., Romano, A., Almasi, B., and Roulin, A. (2025). Real-time context-dependent cooperation in parental provisioning reveals fitness payoffs in barn owls. iScience *28*, 113533. https://doi.org/10.1016/j.isci.2025.113533.

54. Almasi, B., Roulin, A., Jenni-Eiermann, S., and Jenni, L. (2008). Parental investment and its sensitivity to corticosterone is linked to melanin-based coloration in barn owls. Horm. Behav. *54*, 217–223. https://doi.org/10.1016/j.yhbeh.2008.02.021.

55. Dreiss, A.N., and Roulin, A. (2010). Age-related change in melanin-based coloration of barn owls (Tyto alba): females that become more female-like

and males that become more male-like perform better. Biol. J. Linn. Soc. *101*, 689–704. https://doi.org/10.1111/j.1095-8312.2010.01503.x.

56. Roulin, A., Dijkstra, C., Riols, C., and Ducrest, A.-L. (2001). Female- and male-specific signals of quality in the barn owl. J. Evol. Biol. *14*, 255–266. https://doi.org/10.1046/j.1420-9101.2001.00274.x.
57. van den Brink, V., Dreiss, A.N., and Roulin, A. (2012). Melanin-based coloration predicts natal dispersal in the barn owl, Tyto alba. Anim. Behav. *84*, 805–812. https://doi.org/10.1016/j.anbehav.2012.07.001.
58. Bates, D., Mächler, M., Bolker, B., and Walker, S. (2015). Fitting linear mixed-effects models using lme4. J. Stat. Softw. *67*, 1–48. https://doi.org/10.18637/jss.v067.i01.
59. Wood, S.N. (2022). mgcv: Mixed GAM computation vehicle with automatic smoothness estimation. R package. https://cran.r-project.org/package=mgcv.
60. Agostinelli, C., and Lund, U. (2022). circular: Circular Statistics. R Package. https://cran.r-project.org/package=circular.
61. Sumner, M. (2022). traipse: Shared tools for tracking data. R package. https://cran.r-project.org/package=traipse.
62. Thieurmel, B., and Elmarhraoui, A. (2022). suncalc: Compute sun position, sunlight phases, moon position and lunar phase. R package. https://cran.r-project.org/package=suncalc.
63. Dorman, M. (2021). shadow: Geometric shadow calculations. R package. https://cran.r-project.org/package=shadow.
64. Fair, J.M., and Jones, J. (2010). Guidelines to the Use of Wild Birds in Research (Ornithological Council).
65. Frey, C., Sonnay, C., Dreiss, A., and Roulin, A. (2011). Habitat, breeding performance, diet and individual age in Swiss barn owls (Tyto alba). J. Ornithol. *152*, 279–290. https://doi.org/10.1007/s10336-010-0579-8.
66. Roulin, A., and Dijkstra, C. (2003). Genetic and environmental components of variation in eumelanin and phaeomelanin sex-traits in the barn owl. Heredity *90*, 359–364. https://doi.org/10.1038/sj.hdy.6800260.
67. San-Jose, L.M., Ducrest, A.-L., Ducret, V., Simon, C., Richter, H., Wakamatsu, K., and Roulin, A. (2016). MC 1R variants affect the expression of melanocortin and melanogenic genes and the association between melanocortin genes and coloration. Mol. Ecol. *26*, 259–276. https://doi.org/10.1111/mec.13861.
68. R Core Team (2022). R: A Language and Environment for Statistical Computing (R Foundation for Statistical Computing). https://www.r-project.org/.
69. Posit Team (2022). RStudio: Integrated Development Environment for R (Posit Software). https://www.rstudio.com/.

STAR★METHODS

KEY RESOURCES TABLE

REAGENT or RESOURCE	SOURCE	IDENTIFIER
Deposited data		
Barn owls behaviour data	Mendeley Data	10.17632/tvnpvhf2yj.2
R Code	Mendeley Data	10.17632/tvnpvhf2yj.2
Software and algorithms		
R (v4.2.2)	The R Foundation	https://www.r-project.org/
RStudio	Posit Software	https://www.rstudio.com/
lme4 (R package)	Bates et al.[58]	https://cran.r-project.org/package=lme4
mgcv (R package)	Wood[59]	https://cran.r-project.org/package=mgcv
circular (R package)	Agostinelli and Lund[60]	https://cran.r-project.org/package=circular
traipse (R package)	Sumner[61]	https://cran.r-project.org/package=traipse
Moonlit (R package)	Śmielak[19]	https://cran.r-project.org/package=moonlit
suncalc (R package)	Thieurmel and Elmarhraoui[62]	https://cran.r-project.org/package=suncalc
shadow (R package)	Dorman[63]	https://cran.r-project.org/package=shadow

EXPERIMENTAL MODEL AND STUDY PARTICIPANT DETAILS

Ethics Statement

All research procedures complied with the legal and ethical guidelines for wildlife research established by the Swiss Department of Consumer and Veterinary Affairs. Authorization for GPS tagging free ranging barn owls (*Tyto alba*) was granted under permits VD, FR, and BE 3213 and 3571. Capture and ringing were approved by the Swiss Federal Office for the Environment. All biologging devices remained below 5% of body mass, as recommended for avian tracking,[64] and were deployed for short periods (maximum 12 days). Long-term monitoring confirmed that tagged individuals exhibited survival and reproductive success comparable to untagged controls.

Study Area and Tag Deployment

Data were collected from wild barn owls (*Tyto alba*) breeding in nest boxes distributed across the Western Swiss plateau—a heterogeneous, predominantly agricultural region interspersed with small woodlands, hedgerows, and isolated trees. This landscape offers diverse hunting opportunities and variable light conditions, making it well-suited for studying nocturnal foraging behaviour. Between March and August in 2019 and 2020, over 380 nest boxes were regularly monitored for barn owl clutches. Upon detecting a clutch, we applied a standardized monitoring protocol (see Frey et al.[65]) to record brood size, estimate hatch dates, and assess adult plumage coloration. These repeated visits enabled accurate reproductive timing and allowed precise biologging deployment.

Barn owls exhibit strong sexual dimorphism in both behaviour and coloration during the breeding season. Females primarily brood and provision young at the nest, while males conduct ~75% of prey deliveries.[17] Males are generally paler but show greater colour variation,[52,66] white females being rare and reddish males relatively common.[67] To avoid confounds and maximize variation, all behavioural analyses focused exclusively on males.

To monitor barn owls' nightly foraging behaviour, we collected 78 GPS tracks from 69 unique male individuals across two breeding seasons (45 tracks in 2019 and 33 in 2020; Figures 5A and S1). Nine individuals were tracked in both years. Each track corresponded to a single owl's movement across 5–6 consecutive nights. Because nest occupancy, breeding timing, and individual identity could not be determined a priori in this wild population, individuals were equipped opportunistically as clutches were detected rather than randomly assigned.

METHOD DETAILS

Plumage coloration

Plumage coloration was scored visually using an ordinal 8-point scale assessing breast, belly, flanks, and wing undersides, ranging from 1 (dark reddish-brown, hereafter 'red') to 8 (immaculate white). This scale correlates strongly with spectrophotometric measurements of brown chroma[55] and provides a reliable proxy for overall plumage brightness. For analyses, we used the average colour score across all body parts.

Tag deployment

Tracks were recorded using AXY-Trek bio-loggers (Technosmart, Italy) affixed as backpacks using Spectra ribbon harnesses (Bally Ribbon Mills, USA). Devices were deployed ~25 days after the first egg hatched— coinciding with peak male provisioning effort. To minimize disturbance effects, data collection began on night 1 (~24 hours after deployment), following a one-day acclimation period. Loggers were recovered after 10 ± 2 days, yielding 5 ± 1 nights of data per individual.

GPS units recorded location at 1 Hz (one fix per second) from 30 minutes before sunset to 30 minutes after sunrise, covering the entire nocturnal foraging period. Tri-axial accelerometers recorded continuous acceleration at 50 Hz (±16g dynamic range; 10-bit resolution), allowing fine-scale behavioural classification. Integrated pressure sensors recorded barometric changes at 1 Hz (accuracy ±10 mBar; resolution 20 mBar). On average, loggers weighed 12.4 g ± 0.1 g, which represents ~4 ± 1% of owl body mass (Males average body mass 281 ± 16.5 g). Loggers strictly remained within the recommended 5% threshold for minimizing behavioural interference.[64]

Camera trap validation

To validate accelerometer-based hunting success estimates, motion-activated cameras (Reconyx HC500 Hyperfire) were installed at nest entrances. These cameras recorded prey deliveries and independently confirmed successful foraging events,[17] supporting the reliability of acceleration-derived metrics.

Data processing

Hunting event detection

We applied a Boolean-based algorithm[43] to the tri-axial acceleration data to identify hunting events with high precision, enabling detailed analysis of foraging strategies relative to moonlight exposure. Following Schalcher et al.,[17] hunting strikes were defined as rapid descents from flight to ground, characterized by a distinctive acceleration signature marking the final attack phase. Each strike was annotated for outcome (capture vs. miss).

Attack orientation

To estimate attack orientation (in radians), we calculated the bearing from the descent initiation point to the prey location (Figures 5B and 5C). The start of descent was identified from barometric pressure data as the onset of sustained pressure increase (reflecting altitude loss). The prey location was estimated as the median of GPS positions recorded during the stationary phase following each strike. Bearings were computed using the 'track_bearing_to' function from the R package 'traipse' (v. 0.3.0),[61] which robustly estimates directionality between sequential GPS coordinates.

Moonlight intensity

Moonlight intensity at the time and location of each hunting event was estimated using the 'calculateMoonlightStatistics' and 'calculateMoonlightIntensity' functions from the R package *Moonlit*,[19] which incorporate lunar disk brightness and Earth–Moon distance. The output is a continuous, relative moonlight intensity index scaled between 0 and 1, where 1 represents the brightness of a full moon at zenith at mean lunar distance. This standardized metric facilitated cross-event comparison of ambient illumination. In practice, moonlight intensity values observed in our dataset ranged from 0 (Moon below the horizon) to approximately 0.2. For descriptive and visualization purposes (e.g. circular representations), this continuous variable was additionally categorized into three levels—no moonlight (Moon below the horizon), low moonlight (illumination 0–0.09), and high moonlight (> 0.09)—with thresholds defined based on the empirical distribution of illumination values. All statistical models, however, treated lunar illumination as a continuous variable.

Moonlight alignment vector

To quantify the component of moonlight projected along the owl's attack trajectory, we used a vector projection approach to derive a continuous "Moonlight Alignment Vector" (MAV) (Equation 1; Figure 2A). For each hunting attempt, we defined the moonlight vector from the Moon's azimuth and elevation (using 'getMoonPosition' function from the R package *suncalc*, v0.5.1[62]), scaled it by relative moonlight intensity (from R package *Moonlit*[19]), and projected this vector onto the owl's attack vector using

$$MAV = -I \times \cos(\theta) \quad \text{(Equation 1)}$$

I is the moonlight intensity (scaled 0–1), and θ is the angular difference between owl attack direction and incoming moonlight vector. The resulting vector takes positive values when attacks are aligned with incoming moonlight (Moon illuminating owl's frontal body), and negative values when attacks are oriented away from the Moon (Figure 2A).

Shadow mapping

To assess spatial moonlight exposure, we generated high-resolution shadow maps accounting for local topography and vegetation (Figure 3C). For each hunting event, we calculated lunar position and modelled shadows cast by buildings, trees, and forests within a 500 m buffer. Obstacle heights were derived from high-resolution Swiss digital surface models (DSM, Swisstopo). Forests were subdivided into 2 × 2 m grid cells to resolve fine-scale canopy structure.

Shadows were modelled using the 'shadowHeight' function from the R package *shadow* (v0.7.1[63]) which calculates the height of shadow cast on the ground given obstacle height and lunar position. Habitat features were classified using the TLM3D catalogue (1-3 m resolution), and surface elevation and object heights were obtained from swissALTI3D and swissSURFACE3D (both at 0.5m resolution). Final raster maps (5 × 5 m resolution) provided spatially explicit estimates of moonlight exposure, allowing us to classify each hunting attempt as either moonlit or shadowed.

QUANTIFICATION AND STATISTICAL ANALYSIS

Statistical framework

All statistical analyses were conducted in R version 4.2.2[68] using RStudio.[69] We used the packages lme4 (v1.1-27.1[58]) for Linear and Generalized Linear Mixed Models (LMMs and GLMMs), mgcv (v1.8-34[59]) for Generalized Additive Mixed Models (GAMMs), and the circular package (v0.4-95[60]) to analyse angular data.

For continuous and count responses (e.g., projected moonlight, prey capture rate, foraging duration), we fitted LMMs, GLMMs, or GAMMs depending on the response distribution and whether non-linear relationships with illumination were expected. Random intercepts were included for individual identity (Bird ID) and for deployment (TrackID), with deployments nested within individuals. A deployment refers to a continuous recording period of 5–6 consecutive nights during which a single individual carried a bio-logger. This random-effects structure accounts for repeated nightly observations within a single deployment and for repeated measurements of the same individual across deployments or years and was applied consistently across all models.

Model selection focused on the fixed-effect structure and was guided by Akaike Information Criterion (AIC) and biological interpretability. This multi-model framework allowed us to capture non-linear responses to moonlight intensity (via smooth terms in GAMMs), control for repeated sampling inherent to the study design (via random effects), and incorporate interactions between colour morph, illumination, and microhabitat. All predictor variables were checked for multicollinearity using variance inflation factors (VIF), and continuous predictors were centred and scaled prior to modelling to improve interpretability and convergence. Descriptive statistics are reported as mean ± standard deviation (SD), unless otherwise specified. All p-values are two-tailed and statistical significance was assessed at an alpha level of 0.05. We analysed barn owl foraging behaviour using a unified statistical framework encompassing (i) attack orientation, (ii) spatiotemporal moonlight exposure, and (iii) foraging performance outcomes.

Attack orientation

To evaluate whether barn owls oriented their attacks in relation to the Moon, we first described the distribution of attack directions under different moonlight conditions. Attack orientation (in radians) was estimated as the bearing from the descent initiation point to the prey location, as described above. For descriptive circular statistics, we used Rayleigh tests to quantify the degree of directional clustering within each combination of colour morph and moonlight category. Rayleigh tests were conducted separately for white and red morphs, defined as individuals in the upper (colour scores 7.5–8) and lower (scores 1–4.625) quartiles of the continuous plumage scale, respectively, thereby maximizing contrast while retaining adequate sample sizes. We further stratified attacks into three moonlight conditions based on the empirical distribution of illumination values: (1) no moonlight (Moon below horizon), (2) low moonlight (intensity 0–0.09), and (3) high moonlight (intensity > 0.09; maximum ≈ 0.20). For each morph × moonlight combination we report mean direction, mean vector length (R), and associated Rayleigh p-value. Because attacks within individuals and nights are not strictly independent, we use the Rayleigh tests as descriptive summaries of directional bias within morph × moonlight classes. Our main inferential analysis of morph-specific alignment is provided by the mixed-effects MAV model, which quantifies continuously how alignment strength varies across the moonlight gradient and the full plumage-colour continuum.

Alignment to moonlight vector

We modelled moonlight alignment vector (MAV)—defined as the vector of moonlight projected along the owl's attack vector—using a GAMM to test whether plumage coloration modulates the alignment between attacks and lunar illumination across the moonlight gradient. Because residual variance in MAV estimates increased with moonlight intensity (heteroscedasticity), we first fitted a Generalized Least Squares (GLS) model with an exponential variance structure, *varExp(form = ~moonlight intensity)*, including hour of night, moonlight intensity, and plumage coloration as fixed effects. We then used the absolute GLS residuals to derive observation-level weights (inverse of residual magnitude), which down-weighted high-variance observations in the final GAMM and improved model stability.

The final GAMM included plumage coloration, moonlight intensity, year, hour of night, and their interaction (smooth interaction between moonlight intensity and coloration) as fixed effects. This model provides the main inferential test of whether colour morphs differ in their use of attack orientation to modulate moonlight reflection, while Rayleigh statistics provide complementary descriptive information on orientation bias. Only attacks occurring under direct moonlight were included, ensuring that modelled MAV values correspond to biologically relevant illumination.

Spatiotemporal modulation of foraging exposure to moonlight

Moonlight varies across both time and space,[19,20] creating a dynamic nocturnal lightscape. To understand how barn owls exploit these fluctuating conditions, we examined (i) within-night temporal preferences for particular light conditions and (ii) spatial exposure to moonlit versus shaded areas. Together, these analyses quantified how barn owls adjust when and where they hunt in response to the lunar lightscape.

Within-night temporal moonlight preference

To quantify how barn owls selectively adjusted the timing of their hunting activity relative to the nightly lightscape, we calculated a within-night measure of "moonlight preference" for each hunting attempt. Temporal moonlight preference was defined as the relative difference between (i) the moonlight intensity at the time and place of each hunting attempt and (ii) the mean moonlight intensity

available during that individual's active hunting period (time interval between its first and last detected hunting attempt) and spatial range (locations of hunting attempts) on that night. Negative values indicate that the owl hunted during periods that were darker than average illumination it experienced that night, whereas positive values indicate hunting during brighter-than-average periods. This measure therefore captures selection for particular time windows of illumination relative to what was temporally available within the night, rather than selection on absolute moonlight levels. We modelled temporal moonlight preference using a weighted GAMM, allowing for non-linear responses to moonlight. Because the variance of moonlight preference increased with nightly mean illumination, we first fitted a GLS model with an exponential variance structure, *varExp(form = ~nightly mean moonlight intensity)*, including hour of night, plumage coloration, and nightly mean moonlight intensity as fixed effects. Observation-level weights were then computed as the inverse of the absolute GLS residuals and applied to the GAMM.

The final GAMM for temporal preference included Year, hour of night, plumage coloration and nightly mean moonlight intensity as fixed effects. To focus on behavioural responses to direct moonlight, we excluded hunting attempts that occurred when the Moon was below the horizon or in locations where obstacles fully blocked lunar illumination (shadowed areas).

Spatial moonlight exposure

To assess spatial use of moonlit versus shaded areas, we modelled whether each hunting attempt occurred in shadowed (coded 1) or under direct moonlight (coded 0) using a GAMM with a binomial response. Fixed effects included plumage coloration, hunting strategy, hour of night, and nightly mean moonlight intensity. Shadow status was derived from high-resolution spatial maps integrating lunar position, obstacle height, and terrain (see above). Obstacles included forests, trees, and buildings within 500 m of each hunting location. We restricted analyses to nights when the Moon was above the horizon, thereby ensuring that shadow classification reflected biologically meaningful lunar exposure.

Foraging outcomes under moonlight: success, rate, and duration

To test whether behavioural adjustments to moonlight translate into functional foraging differences between colour morphs, we modelled three complementary performance metrics: (1) per-attack hunting success (capture probability), (2) prey capture rate (captures per hour of active hunting), (3) nightly foraging duration (time between first and last hunting attempt).

Per-attack hunting success

We modelled the probability of prey capture at each hunting attempt using a generalized linear mixed model (GLMM) with a binomial error distribution (success = 1, failure = 0). Fixed effects included year, brood size, moonlight intensity, plumage coloration, and the interaction between moonlight intensity and plumage coloration, all treated as continuous predictors to test for morph-specific responses to lunar illumination. We additionally included hunting strategy (aerial vs. sit-and-wait) and moonlight availability at the hunting site (no moonlight, shadowed areas, and directly moonlit areas) as categorical covariates to account for differences in hunting mode and local illumination geometry.

Prey capture rate

Nightly foraging efficiency was quantified as the number of successful captures per hour of active hunting. We modelled prey capture rate using a GAMM with a Tweedie distribution and log link to accommodate zero inflation and continuous positive values. Fixed effects included year, brood size, nightly moonlight intensity, plumage coloration, and their interaction (moonlight $\times$ plumage coloration). To account for variation in nightly foraging effort, we weighted observations by the total number of hunting attempts per night, reducing the influence of nights with unusually low foraging activity.

Foraging Duration

Nightly foraging duration (time between the first and the last hunting) was modelled using an LMM. Fixed effects included year, moonlight intensity, brood size, overall activity level, and the interaction between moonlight intensity and plumage coloration. This model evaluates whether any advantages in prey capture rate under bright conditions are accompanied by reductions in nightly foraging time, consistent with more efficient provisioning during moonlit periods.

Current Biology, Volume *36*

Supplemental Information

Barn owl color morphs hunt differently in moonlight

Kim Schalcher, Estelle Milliet, Robin Séchaud, Roman Bühler, Bettina Almasi, Paolo Becciu, and Alexandre Roulin

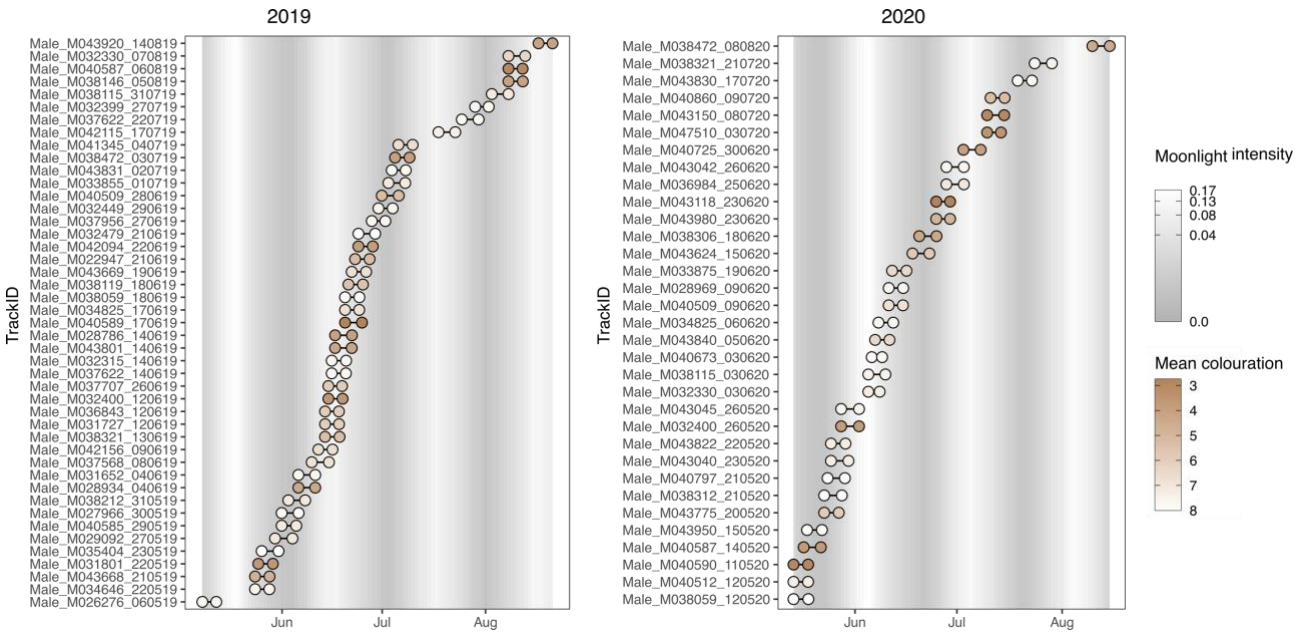


Figure S1. Temporal distribution of tracking sessions. Related to Figures 1 and 4. Temporal distribution of the 78 tracking sessions recorded from 69 male barn owls in the study population in 2019 (left panel) and 2020 (right panel). Each horizontal line represents one tracking session, extending from its start to its end. Circles at both ends mark the beginning and end of the session. Circle fill color indicates male plumage coloration, ranging from white to reddish-brown. Background shading indicates moonlight illumination through time, with darker grey corresponding to lower illumination and lighter shading to higher illumination.

LME **Moonlight alignment vector**

Term	Estimate	Std. Error	t-value	p-value
Intercept	0.0003	0.0020	0.1478	0.8825
Year2020	0.0001	0.0009	0.0410	0.9673
hour of the night	0.0001	0.0001	0.7653	0.4441
mean coloration	0.0011	0.0003	3.3099	**0.0009**

GAM

Term	EDF	F-value	p-value
s(moonlight): mean coloration	3.39	23.21	**<0.001**
Observations			7704
R^2			0.092

Table S1. Effect of moonlight and plumage coloration on moonlight alignment vector (MAV) during barn owl attacks. Related to Figure 3. Summary of a Generalized Additive Mixed Model (GAMM) evaluating variation in the moonlight alignment vector (MAV) during attacks. MAV was defined as the projected intensity of moonlight along the owl's attack trajectory, with positive values indicating reflection toward the prey and negative values indicating reflection away. Fixed effects included hour of the night and plumage coloration (modelled linearly), and a non-linear interaction between moonlight intensity and plumage coloration modelled as an additive smooth term. Random intercepts for Bird ID and deployment (TrackID, nested within Bird ID) were included to account for the hierarchical structure of the data. To correct for heteroscedasticity, model weights were derived from a prior Generalized Least Squares (GLS) model with an exponential variance structure. Reported outputs include linear predictor estimates (LME), effective degrees of freedom (EDF), F-values, and p-values for the smooth term. EDF values quantify the degree of non-linearity in the moonlight x coloration interaction. The analysis is based on 7,704 hunting attempts across 78 tracks from 69 individuals.

LME **Moonlight preference**

Term	Estimate	Std. Error	t-value	p-value
Intercept	0.0001	0.0001	-1.2941	0.1956
hour of the night	0.0005	0.0000	13.2657	**<0.001**
Year (2020)	0.0001	0.0001	0.4344	0.664
mean coloration	0.0002	0.0004	0.5273	0.598

GAM

Term	EDF	F-value	p-value
s(mean moonlight): mean coloration	4.47	157.80	**<0.001**
Observations			17,039
R^2			0.222

Table S2. Effect of moonlight and plumage coloration on moonlight preference during barn owl attacks. Related to Figure 4. Summary of the Generalized Additive Mixed Model (GAMM) assessing variation in moonlight preference, defined as the deviation between the moonlight intensity at each hunting attempt and the nightly average moonlight available. Positive values indicate selection for brighter periods within the night; negative values indicate selection for darker intervals. Hour of the night and plumage coloration were included as linear fixed effects, with a non-linear interaction between moonlight intensity and plumage coloration modelled as an additive smooth term. Random intercepts for Bird ID and deployment (TrackID, nested within Bird ID) were included to account for the hierarchical structure of the data. To address heteroscedasticity, model weights were derived from a preceding Generalized Least Squares (GLS) model with an exponential variance structure. Reported outputs include linear predictor estimates, effective degrees of freedom (EDF), F-values, and p-values for the smooth terms. EDF values reflect the degree of non-linearity in the moonlight x coloration interaction. The analysis includes 17,039 hunting attempts across 78 tracks from 69 individuals.

LME	Probability of hunting in shadowed ground			
Predictors	Estimate	Std. Error	z-value	p-value
Intercept	-1.9874	0.5029	-3.9461	**<0.001**
Mean coloration	0.1896	0.1247	1.5207	0.1283
Hour of the night	-0.0053	0.0267	-0.1992	0.8421
Hunting strategy (perching)	0.6183	0.1008	6.1337	**<0.001**

GAM

Predictors	EDF	Chi2	p-value
s(Moonlight) : mean coloration	3.71	152.78	**<0.001**
Observations			7,348
R^2			0.122

Table S3. Effect of moonlight and plumage coloration on the probability of hunting in shadowed ground. Related to Figure 4. Summary of a binomial Generalized Additive Mixed Model (GAMM) evaluating the probability that barn owl hunting attempts occurred in shadowed ground (coded as 1) versus moonlight-exposed ground (coded as 0). Shadowed areas were defined as locations not directly illuminated by moonlight due to environmental obstacles such as vegetation or buildings. Fixed effects included plumage coloration, hour of the night, and hunting strategy (linear terms), along with a non-linear interaction between moonlight intensity and plumage coloration modelled as an additive smooth term. Random intercepts for Bird ID and deployment (TrackID, nested within Bird ID) were included to account for the hierarchical structure of the data. Reported outputs include linear predictors, effective degrees of freedom (EDF), chi-squared statistics, and p-values for the smooth term. EDF reflects the degree of non-linearity in the moonlight x coloration interaction. The analysis is based on 7,348 hunting attempts across 76 tracks from 67 individual barn owls.

GLMM	**Hunting success**		
Predictors	*Odds Ratios*	*CI*	*p*
Intercept	0.33	0.30 – 0.36	**<0.001**
Hunting strategy (sit-and-wait)	1.29	1.17 – 1.42	**<0.001**
Moonlight	0.95	0.90 – 1.01	0.058
Year (2020)	1.05	0.95 – 1.21	0.495
Mean coloration	0.98	0.90 – 1.06	0.605
Brood size	1.06	0.99 – 1.14	0.103
Light availability (shadowed areas)	1.08	0.91 – 1.28	0.394
Light availability (moonlit light)	1.13	1.03 – 1.25	**0.012**
Moonlight : mean coloration	1.02	0.96 – 1.08	0.550
Light availability (shadowed areas) : mean coloration	0.92	0.79 – 1.09	0.346
Light availability (moonlit light) : mean coloration	1.03	0.93 – 1.13	0.617
Observations		17,601	
Marginal R^2 / Conditional R^2		0.005 / 0.025	
Random Effects: σ^2 = 3.29 | ICC = 0.02 | N_{BirdID} = 67 | $N_{TrackID}$ = 77			

Table S4. Effect of moonlight and plumage coloration on per-attack hunting success in barn owls. Related to Figure 5. Summary of a binomial Generalized Linear Mixed Model (GLMM) evaluating the probability of successful prey capture during individual hunting attempts (success = 1; failure = 0). Fixed effects included standardized moonlight intensity, plumage coloration, brood size, year, and the interaction between moonlight intensity and plumage coloration. Random intercepts for Bird ID and deployment (TrackID, nested within Bird ID) were included to account for the hierarchical structure of the data. The model is based on 18,425 hunting attempts across 77 tracks from 67 individual barn owls. Reported results include odds ratios (OR) with 95% confidence intervals (CI) and associated p-values for fixed effects. Marginal and conditional R^2 values are provided to indicate the variance explained by fixed effects alone and by the full model, respectively. Random effect variance (σ^2) and the intraclass correlation coefficient (ICC) are reported at the bottom of the table.

LME	Nightly prey capture rate (prey*h^{-1})			
Predictors	Estimate	Std. Error	t-value	p-value
Intercept	0.5434	0.1897	2.8653	**0.0045**
Brood size	0.0128	0.0292	0.4399	0.6603
Year (2020)	0.1228	0.0785	1.5639	0.119
Mean coloration	0.0027	0.0240	0.1118	0.9111

GAM

Predictors	EDF	F-value	p-value
s(mean moonlight) : mean coloration	3.93	367.09	**<0.001**
Observations			354
R^2			0.435

Table S5. Effect of moonlight and plumage coloration on nightly prey capture rate in barn owls. Related to Figure 5. Summary of a Generalized Additive Mixed Model (GAMM) evaluating variation in prey capture rate per hour of foraging (prey·h^{-1}) as a function of moonlight intensity and plumage coloration. Year and brood size were included as additional linear fixed effects, and the interaction between moonlight intensity and plumage coloration as a smooth term. Random intercepts for Bird ID and deployment (TrackID, nested within Bird ID) were included to account for the hierarchical structure of the data. Observations were weighted by the total number of hunting attempts per night to account for variation in foraging effort and improve estimation robustness. The model employed a Tweedie distribution with a log link to accommodate zero-inflated and right-skewed count data. Reported results include linear predictor estimates, effective degrees of freedom (EDF), F-values, and p-values for the smooth term. The analysis is based on 354 nights across 77 tracks from 67 individual barn owls.

GLMM	Nightly foraging duration (h)		
Predictors	*Estimates*	*CI*	*p*
Intercept	5.40	4.78 – 6.02	**<0.001**
Brood size	0.07	-0.01 – 0.15	0.105
Year (2020)	-0.09	-0.30 – 0.12	0.402
Hunting activity	0.01	0.01 – 0.02	**<0.001**
Mean moonlight	11.92	0.48 – 23.36	**0.041**
Mean coloration	-0.03	-0.11 – 0.05	0.507
Mean moonlight : mean coloration	2.44	0.62 – 4.27	**0.009**
Observations	354		
Marginal R^2 / Conditional R^2	0.151 / 0.419		
Random Effects: σ^2 = 0.36 | ICC = 0.32 | N_{BirdID} = 67 | $N_{TrackID}$ = 77			

Table S6. Effect of moonlight and plumage coloration on nightly foraging duration in barn owls. Related to Figure 5. Summary of a Linear Mixed-Effects Model (LMM) evaluating variation in nightly foraging duration (hours) as a function of moonlight intensity, plumage coloration, and their interaction. Additional fixed effects included brood size, year, and total hunting effort (number of hunting attempts). Random intercepts for Bird ID and deployment (TrackID, nested within Bird ID) were included to account for the hierarchical structure of the data. Reported estimates include 95% confidence intervals and associated p-values. Marginal and conditional R^2 values indicate variance explained by fixed effects alone and by the full model (fixed and random effects), respectively. Random effect variance (σ^2) and the intraclass correlation coefficient (ICC) are reported at the bottom of the table. The analysis is based on 354 nights across 77 tracks from 67 individual barn owls.